

Original Article

Atorvastatin Slows the Progression of Cardiac Remodeling in Mice with Pressure Overload and Inhibits Epidermal Growth Factor Receptor Activation

Yulin LIAO¹), Hui ZHAO²), Akiko OGAI¹), Hisakazu KATO²), Masanori ASAKURA¹), Jiyoung KIM¹), Hiroshi ASANUMA¹), Tetsuo MINAMINO²), Seiji TAKASHIMA²), and Masafumi KITAKAZE¹)

The aim of this study was to investigate whether atorvastatin inhibits epidermal growth factor receptor (EGFR) activation in cardiomyocytes *in vitro* and slows the progression of cardiac remodeling induced by pressure overload in mice. Either atorvastatin (5 mg/kg/day) or vehicle was orally administered to male C57BL/6J mice with transverse aortic constriction (TAC). Physiological parameters were obtained by echocardiography or left ventricular (LV) catheterization, and morphological and molecular parameters of the heart were also examined. Furthermore, cultured neonatal rat cardiomyocytes were studied to clarify the underlying mechanisms. Four weeks after TAC, atorvastatin reduced the heart/body weight and lung/body weight ratios (8.69 ± 0.38 to 6.45 ± 0.31 mg/g ($p < 0.001$) and 10.89 ± 0.68 to 6.61 ± 0.39 mg/g ($p < 0.01$) in TAC mice with and without atorvastatin, respectively). Decrease of LV end-diastolic pressure and the time constant of relaxation, increased fractional shortening, downregulation of a disintegrin and metalloproteinase (ADAM)12, ADAM17 and heparin-binding epidermal growth factor genes, and reduction of the activity of EGFR and extracellular signal-regulated kinase (ERK) were observed in the atorvastatin group. Phenylephrine-induced protein synthesis, phosphorylation of EGFR, and activation of ERK in neonatal rat cardiomyocytes were all inhibited by atorvastatin. These findings indicated that atorvastatin ameliorates cardiac remodeling in mice with pressure overload, and its actions are associated with inhibition of the EGFR signaling pathway. (*Hypertens Res* 2008; 31: 335–344)

Key Words: statins, epidermal growth factor receptor, heart failure, hypertrophy, extracellular signal-regulated kinase

Introduction

Although substantial evidence obtained by various clinical trials has demonstrated the efficacy of β -blockers, angio-

tensin-converting enzyme inhibitors, angiotensin receptor blockers, aldosterone antagonists, and vasodilators for treatment of chronic heart failure (CHF) (1), the mortality and morbidity of this serious condition remain high. Therefore, investigation of novel treatments to improve the prognosis of

From the ¹Cardiovascular Division of Medicine, National Cardiovascular Center, Suita, Japan; and ²Department of Cardiovascular Medicine, Osaka University Graduate School of Medicine, Suita, Japan.

This work was supported by Grants (H13-Genome-011 and H13-21seiki (seikatsu)-23) from the Japanese Ministry of Health, Labour and Welfare. One of the authors (Y.L.) was supported by a grant from the Japan Society for the Promotion of Science (P05228).

Address for Reprints: Masafumi Kitakaze, M.D., Ph.D., Cardiovascular Division of Medicine, National Cardiovascular Center, 5-7-1 Fujishirodai, Suita 565-8565, Japan. E-mail: kitakaze@z66.so-net.ne.jp

Received April 5, 2007; Accepted in revised form September 2, 2007.

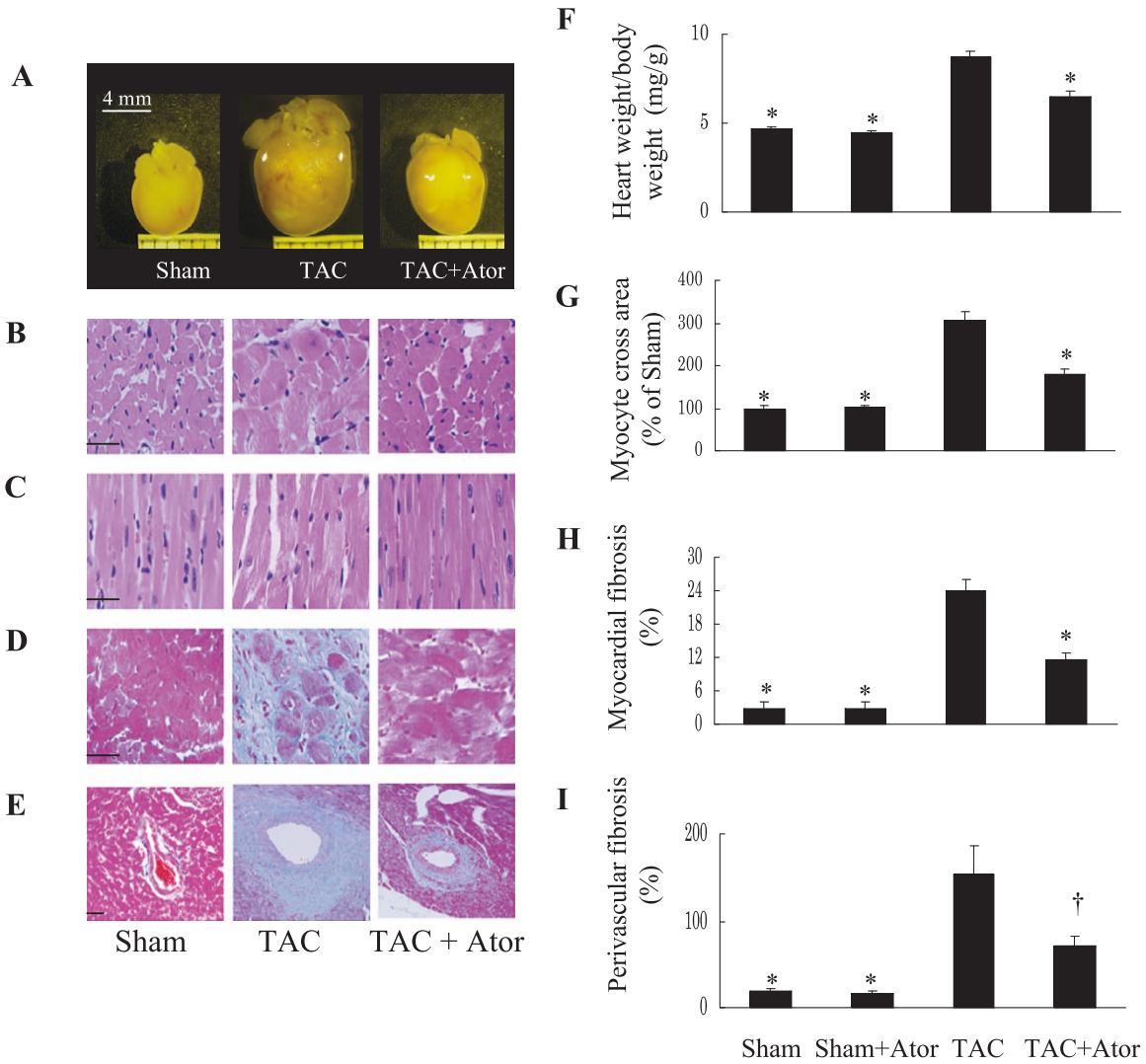


Fig. 1. Effect of atorvastatin (Ator) on cardiac hypertrophy and fibrosis in mice with pressure overload. *A:* Representative pictures of the whole heart. *B:* Cardiomyocyte cross-sectional surface area (hematoxylin and eosin stain [H&E stain]). *C:* Long-axis view of cardiomyocytes (H&E stain). Myocardial fibrosis (*D*) and perivascular fibrosis (*E*) are revealed by Azan staining. The heart weight/body weight ratio (HW/BW, ANOVA $p < 0.0001$) (*F*) and cardiomyocyte cross-sectional surface area (ANOVA $p < 0.0001$) (*G*) were significantly reduced in atorvastatin-treated mice. Myocardial fibrosis (ANOVA $p < 0.0001$) (*H*) and perivascular fibrosis (ANOVA $p < 0.003$) (*I*) were also inhibited by atorvastatin. * $p < 0.01$, † $p < 0.05$ vs. TAC by post-hoc test. In *F*, the number of mice is 12, 5, 12 and 11 for the sham, sham+Ator, TAC, and TAC+Ator groups, respectively. In *G–I*, 3–5 hearts from each group were used to obtain data. Bar: 20 μm .

CHF is an area of intense activity. Recent clinical studies performed by us as well as others have shown that hydroxymethylglutaryl-CoA (HMG-CoA) reductase inhibitors (statins) improve cardiac remodeling and survival in patients with either ischemic or non-ischemic CHF (2–5), suggesting that statin therapy may be a potential new approach for CHF. Randomized double-blind placebo-controlled trials that are still ongoing (6, 7) may eventually provide firm evidence about this issue. In the meantime, well-designed experimental studies will also be helpful to clarify whether statins are beneficial

for both systolic and diastolic heart failure, as well as to explore the underlying mechanisms.

Theoretically, several of the many actions of statins may contribute to the improvement of cardiac remodeling. Our previous study demonstrated that myocardial hypertrophy can be induced *via* activation of matrix metalloproteinases (MMPs), which is followed by the subsequent release of heparin binding–epidermal growth factor (HB-EGF) and phosphorylation of the epidermal growth factor receptor (EGFR), and we have shown that an MMP inhibitor can ameliorate

Table 1. Echocardiographic Findings at 4 Weeks after TAC or Sham Operation

Parameters	Sham (n=10)	Sham+Ator (n=5)	TAC (n=11)	TAC+Ator (n=11)	ANOVA p value
LVEDd (mm)	2.85±0.05*	2.89±0.08 [#]	3.22±0.07	2.89±0.05*	0.004
LVPWd (mm)	0.65±0.01* [†]	0.61±0.02* [†]	0.92±0.02	0.74±0.02*	<0.0001
LVESd (mm)	1.20±0.06*	1.39±0.12*	2.10±0.1	1.15±0.09*	<0.0001
LVFS (%)	58±2*	52±3*	35±2	60±3*	<0.0001
LVEF (%)	89±1*	89±3*	65±3	89±2*	<0.0001
HR (bpm)	543±11	540±10	490±27	527±28	0.492

TAC, transverse aortic constriction; Ator, atorvastatin; LVEDd, left ventricular end-diastolic dimension; LVPWd, left ventricular diastolic posterior wall thickness; LVESd, left ventricular end-systolic dimension; LVFS, left ventricular fractional shortening; LVEF, left ventricular ejection fraction; HR (bpm), heart rate (beats per minute). * $p < 0.01$, [#] $p < 0.05$ compared with TAC, [†] $p < 0.01$ vs. TAC+Ator. Data are mean±SEM.

cardiac hypertrophy and improve heart failure (8). However, it remains unknown whether or not statins inhibit this signal pathway.

Atorvastatin is the most frequently prescribed statin worldwide, but few studies have been performed to clarify its influence on the progression of non-ischemic CHF and the possible cellular mechanisms involved. Accordingly, we investigated whether atorvastatin had a beneficial effect on the morphology and function of the left ventricle in mice with pressure overload, and we also investigated whether inhibition of EGFR activation had a role in the beneficial effects of statin therapy. We found that atorvastatin slowed the progression of cardiac remodeling and inhibited the activation of EGFR and extracellular signal-regulated kinase (ERK).

Methods

Transverse Aortic Constriction Model and Experimental Protocol

All procedures were performed in accordance with our institutional guidelines for animal research, which conform to the "Guide for the Care and Use of Laboratory Animals" published by the US National Institutes of Health (NIH Publication No. 85-23, revised 1996). Male C57BL/6J mice (7–8 weeks old and weighing 20–24 g) were anesthetized with a mixture of intraperitoneal xylazine (5 mg/kg) and ketamine (100 mg/kg). Transverse aortic constriction (TAC) was performed to induce cardiac hypertrophy and heart failure, as described previously (9, 10).

Mice were divided into 4 groups, which were the sham ($n=12$), sham+atorvastatin ($n=9$), TAC ($n=13$), and TAC+atorvastatin ($n=12$) groups. Atorvastatin calcium (an HMG-CoA reductase inhibitor kindly provided by Pfizer Pharmaceutical Co., Ltd., Tokyo, Japan) was administered at a daily dose of 5 mg/kg (dissolved in 10% ethanol and orally administered by gavage) from day 2 after TAC. The dose of atorvastatin was determined according to a previous report (11). After echocardiography and left ventricular (LV) hemo-

dynamic studies were done at 4 weeks following TAC, the mice were sacrificed and their hearts and lungs were extracted for further analysis. For histological examination, hearts were fixed in 10% formalin and stained with hematoxylin/eosin or Azan/Mallory, whereas the hearts used for Western blot analysis were snap-frozen in liquid nitrogen and stored at -80°C until use. Hearts for RNA analysis were stored in RNAlater liquid.

Echocardiography

Transthoracic echocardiography was performed with a Sonos 4500 and a 15-6L MHz transducer (Philips, Eindhoven, the Netherlands). Mice were fixed in position without anesthesia. Two-dimensional short-axis views of the left ventricle were obtained for guided M-mode measurement of the posterior wall thickness (LVPWd), end-diastolic dimension (LVEDd), and end-systolic dimension (LVESd). LV fractional shortening (FS) and the ejection fraction (EF) were calculated as follows:

$$\text{LVFS} = (\text{LVEDd} - \text{LVESd}) / \text{LVEDd} \times 100,$$

$$\text{LVEF} = [(\text{LV end-diastolic volume} - \text{LV systolic volume}) / \text{LV end-diastolic volume}] \times 100.$$

The LV volume was calculated by the formula of Teichholz:

$$V = [7 / (2.4 + D)] \times D^3,$$

where V is the LV volume and D is the LV dimension (12).

Invasive Hemodynamic Study

LV hemodynamics were evaluated at 4 weeks after TAC. Mice from each group were anesthetized (lightly for TAC mice) and were ventilated as mentioned above. A Millar catheter was inserted *via* the right carotid artery and carefully introduced into the left ventricle to measure the systolic pressure (LVSP) and end-diastolic pressure (LVEDP). Maximum and minimum rates of LV pressure change (max dP/dt and min dP/dt , respectively) as well as the contractility index (max dP/dt divided by the pressure at the time of max dP/dt)

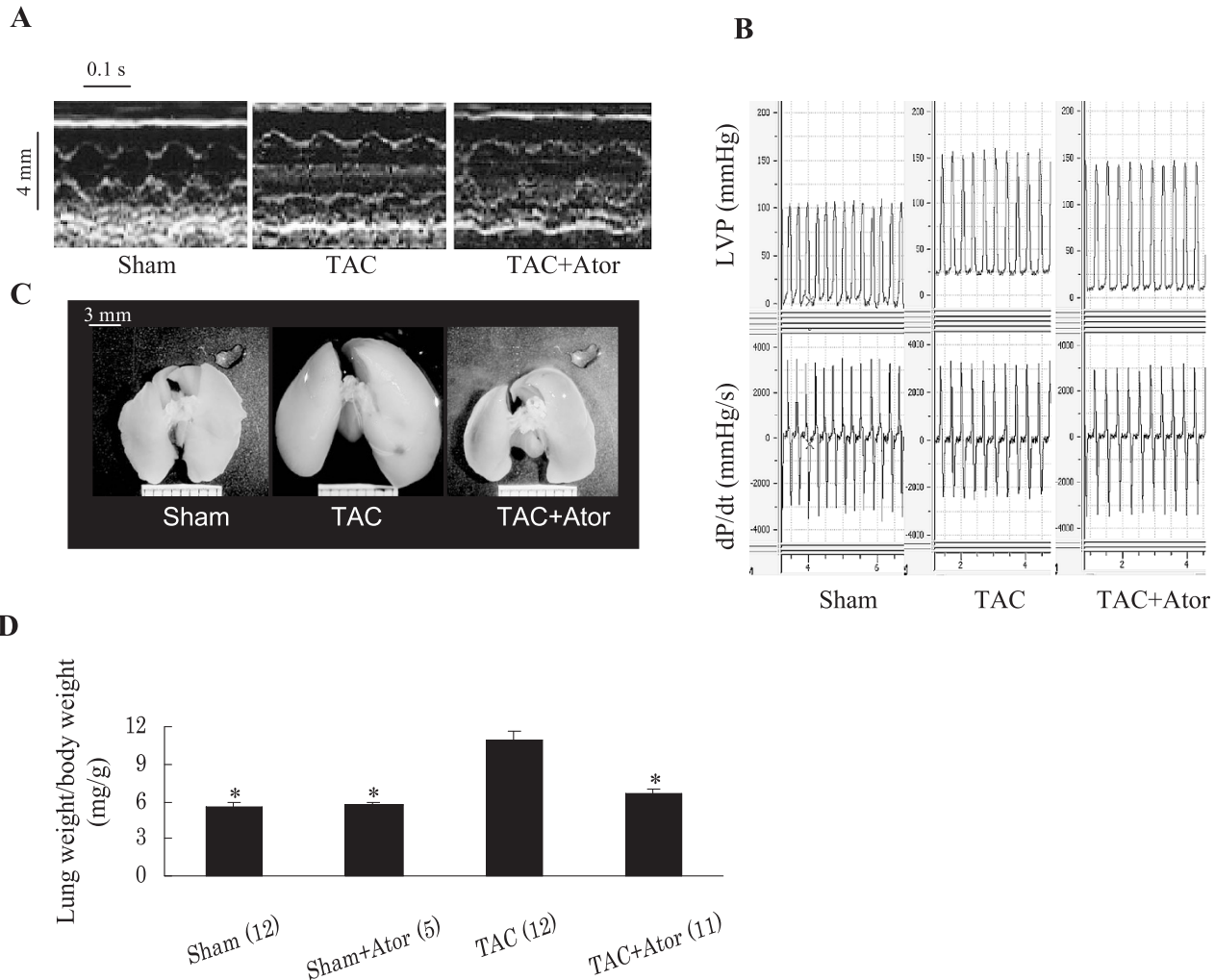


Fig. 2. Improvement of cardiac function by atorvastatin (Ato). *A:* Representative M-mode echocardiographic images. *B:* Representative graph of left ventricular pressure and its rate of change (dP/dt), a lower end-diastolic pressure and higher min dP/dt were seen in the atorvastatin-treated mouse. *C:* Pulmonary congestion was ameliorated by atorvastatin at 4 weeks after TAC. *D:* The lung weight/body weight ratio (LW/BW) was significantly lower in atorvastatin-treated mice than in untreated TAC mice. ANOVA $p < 0.0001$; * $p < 0.01$ vs. TAC. The number of mice is shown in the parentheses.

and the exponential time constant of relaxation (τ) were calculated using a software program (Blood Pressure Module).

Cell Culture

Ventricular myocytes were isolated from neonatal rats at 2 to 3 days of life and cultured as described previously (8). In brief, the cardiomyocytes were incubated for 72 h in Dulbecco's modified Eagle's medium supplemented with 10% fetal calf serum and then grown for 48 h under serum-free conditions. Subsequently, the cells were exposed to phenylephrine (PE, 10^{-4} mol/L) for 24 h in the presence or absence of atorvastatin (10^{-7} to 10^{-5} mol/L). Cellular protein synthesis was evaluated on the basis of [3 H]leucine incorporation and EGFR activation was examined by immunoprecipitation

Western blotting. To examine the effect of atorvastatin or the EGFR inhibitor AG1478 on ERK activation induced by PE, myocytes were exposed to PE 10^{-4} mol/L for 5 min with or without pretreatment for 30 min by atorvastatin 10^{-5} mol/L or AG1478 10^{-6} mol/L.

EGFR Phosphorylation

Cultured cardiomyocytes were exposed to 10^{-4} mol/L PE for 5 min with or without pretreatment for 30 min by atorvastatin (10^{-5} or 10^{-7} mol/L). Then the cells were lysed by incubation for 20 min at 4°C in a buffer (50 mmol/L Tris-HCl, pH 7.3; 150 mmol/L NaCl; 2 mmol/L EDTA; 0.5% sodium fluoride; 10 mmol/L sodium pyrophosphate; 0.5 mmol/L Na_3VO_4 ; 100 $\mu\text{g}/\text{mL}$ phenylmethylsulfonyl fluoride; 2 $\mu\text{g}/\text{mL}$ aprotinin;

Table 2. Left Ventricular Hemodynamics at 4 Weeks after TAC or Sham Operation

Group	LVSP (mmHg)	LVEDP (mmHg)	Max dP/dt (mmHg/s)	Min dP/dt (mmHg/s)	Contractility index	τ (ms)
Sham	86±2.6* [†]	8.3±1.6* [†]	3,074±344	2,695±270 [‡]	77.3±5.5*	19.2±1.3 [#]
Sham+Ator	87±5.1* [†]	5.8±2.3* [†]	3,129±194	2,789±109	79.6±7.5 [#]	17.0±0.5*
TAC	156±3.2	26.0±1.8	3,181±124	3,051±180	45.2±2.5	23.9±1.3
TAC+Ator	163±9.5	16.6±1.8*	3,419±256	3,671±251	66.0±9.1 [#]	18.6±0.4*
ANOVA <i>p</i>	<0.0001	<0.0001	0.7800	0.0033	0.0236	0.0010

TAC, transverse aortic constriction; Ator, atorvastatin, 5 mg/kg/day; LVSP, maximum left ventricular systolic pressure; LVEDP, left ventricular end-diastolic pressure; Max dP/dt, the steepest slope during the upstroke of the pressure curve; Min dP/dt, the steepest slope during the downstroke of the pressure curve; Contractility index, max dP/dt divided by the pressure at the time of max dP/dt; τ , the exponential time constant of relaxation. **p*<0.01, [#]*p*<0.05 vs. TAC, [†]*p*<0.01, [‡]*p*<0.05 vs. TAC+Ator. The number of mice is 10 in each group except for Sham+Ator group (*n*=5). Data are mean±SEM.

protease inhibitor cocktail; and 1% Nonidet P-40). Immunoprecipitation of about 300 μ g protein with Protein G Sepharose 4 Fast Flow (GE Healthcare, Uppsala, Sweden) and an antibody directed against the EGFR (Santa Cruz Biotechnology, Santa Cruz, USA; 1:100), immunoblotting using anti-PY20 to detect phosphorylation (BD Biosciences, San Jose, USA; 1:2,500) and anti-EGFR (Upstate Biotechnology, Lake Placid, USA; 1:500) to determine the EGFR expression were performed as described elsewhere (8).

In vivo EGFR phosphorylation was examined according to a previously described method (13) with some modifications. Briefly, mice were anesthetized with pentobarbital sodium (50 mg/kg). Phosphate buffer solution (10 mL) was perfused into the LV chamber of living hearts and then the heart was extracted and homogenized promptly in lysis buffer on ice. After centrifugation at 15,000 rpm for 10 min, the protein content in the supernatant was quantified and about 8,000 μ g protein for each mouse was immunoprecipitated with Protein G Sepharose 4 Fast Flow and anti-EGFR (Santa Cruz Biotechnology; 1:100), and immunoblotting using anti-PY20 (BD Bioscience, 1:1,000) and anti-EGFR (Upstate, 1:500) were performed.

Western Blot Analysis

Proteins were prepared from whole heart homogenates or cultured cardiomyocytes as described elsewhere (14). Immunoblotting was then performed using a mouse monoclonal antibody directed against ERK1/2 or anti-phospho-ERK1/2 antibodies (Santa Cruz Biotechnology). Immunoreactive bands were visualized by the enhanced chemiluminescence method (Amersham Biosciences, Buckinghamshire, UK) and then were quantified by densitometry with Scion Image software.

Polymerase Chain Reaction

Total RNA was prepared from homogenized whole mouse hearts using RNA-Bee isolation reagent (Tel-Test Inc., Friendswood, USA) according to the manufacturer's proto-

col. The reverse transcription (RT)–polymerase chain reaction (PCR) was performed to generate cDNA from the extracted RNA. Expression quantitation of the genes for HB-EGF, MMP2, and MMP9 and brain natriuretic peptide (BNP) was determined using the TaqMan real-time PCR assay and an ABI PRISM7700 Sequence Detection System (Applied Biosystems, Foster City, USA), as described elsewhere (9). Oligonucleotide primers and TaqMan probes for mouse HB-EGF, MMP2, MMP9, BNP, and RNA 18S were all purchased from Applied Biosystems. Expression of a disintegrin and metalloproteinase (ADAM) 12 (primers: sense 5'-GACTCA TTGCCAATGGCTTCACGGA-3', antisense 5'-ACTCAT GGAGCCTGGTGAATGGGTC-3'), and ADAM17 (primers: sense 5'-ACTGACAAGTCAAGGTGTGCT-3', antisense 5'-TCCTGGATGGTGTCCATCCTCTGGT-3') was detected by regular PCR.

Measurement of Plasma Nitric Oxide

Blood was obtained from the right ventricle with a 25-gauge needle at the time of sacrificing the mice. The plasma concentrations of NO_x (NO₂+NO₃) were measured with an autoanalyzer (ENO-10; Eicom Co., Kyoto, Japan), as described elsewhere (15–17). Samples were applied to an analytical column that was connected to a copperized cadmium reduction column to reduce NO₂ to NO₃, which was then reacted with Griess reagent, and the absorbance of the product was measured at 540 nm.

Statistical Analysis

The unpaired Student's *t*-test was used for comparisons between two groups, while one-way ANOVA with post hoc analysis by the Tukey-Kramer or Fisher test was employed for multiple comparisons. Skewed data were log-transformed or log plus square root-transformed before testing was performed. Results were expressed as the means±SEM and values of *p*<0.05 were considered to indicate statistical significance.

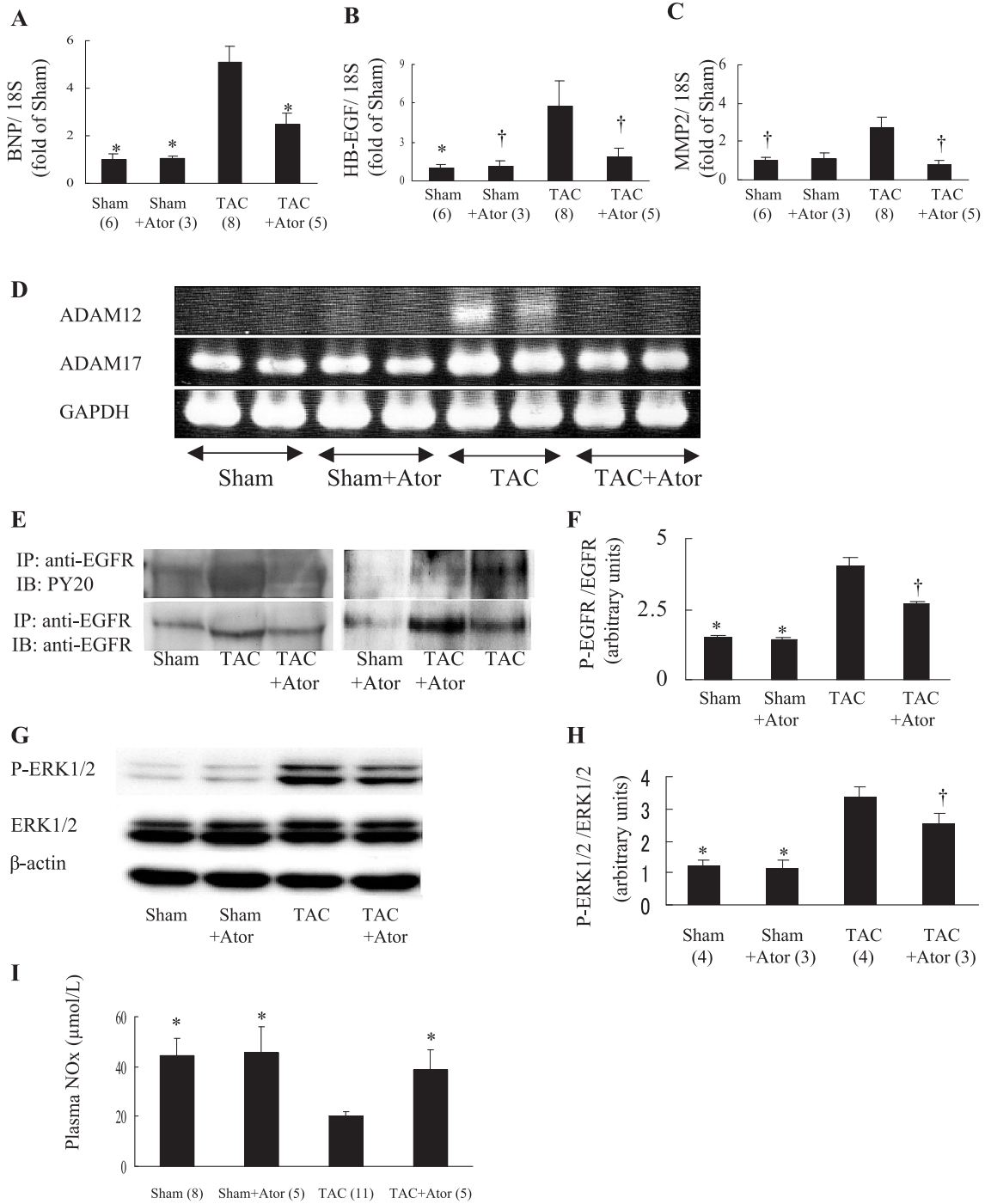


Fig. 3. Atorvastatin (*Ator*) downregulated the expression of natriuretic peptide precursor type B (BNP), heparin-binding epidermal growth factor (HB-EGF), matrix metalloproteinases (MMPs), and EGFR and ERK1/2 activity in *in vivo* experiments. *A–C:* Expressions of the BNP, HB-EGF, and MMP2 genes were evaluated by TaqMan real-time quantitative PCR with 18S RNA as the internal control (ANOVA *p* values were <0.0001, 0.0012 and 0.0126, respectively). **p* < 0.01, †*p* < 0.05 vs. TAC (statistical analysis for HB-EGF was performed after a log and square root transformation). The number of heart samples is shown in the parentheses. *D:* PCR results of ADAM12 and 17. *E:* Representative immunoblot of phospho-EGFR (P-EGFR) and EGFR. *F:* Ratio of P-EGFR to EGFR significantly increased in the hearts of TAC mice, while atorvastatin decreased it. *G:* Western blotting results of phospho-ERK1/2 (P-ERK1/2) and ERK1/2. *H:* Ratio of P-ERK1/2 to ERK1/2 markedly increased in the hearts of TAC mice, while atorvastatin decreased the ratio, β -actin served as the loading control (ANOVA *p* value <0.001). *I:* Plasma nitric oxide levels (ANOVA *p* value <0.0001). **p* < 0.01, †*p* < 0.05 vs. TAC.

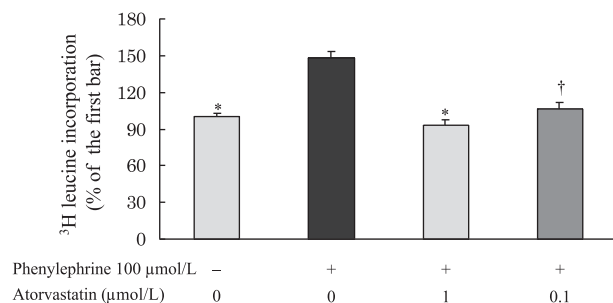


Fig. 4. Atorvastatin inhibited protein synthesis of cultured neonatal rat cardiac myocytes. Phenylephrine enhanced protein synthesis and atorvastatin blocked this action. Each experiment was repeated at least 3 times. The first bar from the left side of the figure served as the control. ANOVA $p < 0.0001$; * $p < 0.01$, † $p < 0.05$ vs. phenylephrine alone.

Results

Atorvastatin Ameliorates Cardiac Hypertrophy

Four weeks after TAC, the wet heart/body weight ratio (HW/BW) and cardiomyocyte cross-sectional surface area were increased in the TAC group compared with the sham group. No significant difference in heart weight was observed between the sham and sham+atorvastatin groups (Fig. 1F). Treatment with atorvastatin (TAC+atorvastatin group) ameliorated the hypertrophy of cardiomyocytes (Fig. 1A–C, F and G). We also observed an inhibitory effect of atorvastatin on myocardial and perivascular fibrosis (Fig. 1D, E, H and I). These findings indicate that atorvastatin therapy was able to inhibit cardiac hypertrophy and fibrosis in mice with LV pressure overload.

Atorvastatin Slows the Onset of Heart Failure

Echocardiographic examination of conscious mice showed a significant increase of LVFS and LVEF, as well as a smaller LV chamber and thinner LV walls, in the TAC+atorvastatin group than in the TAC group (Table 1 and Fig. 2A), suggesting that atorvastatin both improved LV systolic function and inhibited LV remodeling.

We evaluated LV hemodynamics using a Millar pressure catheter before sacrificing the mice. LV pressure overload was similar in the TAC groups with and without atorvastatin treatment (Fig. 2B), but atorvastatin therapy increased the contractility index, in addition to decreasing LVEDP and τ (Table 2), indicating improvement of both systolic and diastolic function.

We have previously demonstrated that pulmonary edema is a reliable index of cardiac function in this model (10, 18, 19). Compared with that in sham mice, the lung/body weight ratio

(LW/BW) was increased by 93% in TAC mice, whereas there was only a 17% increase of the LW/BW in the TAC+atorvastatin group (Fig. 2C, D).

No significant differences in the above-mentioned parameters were noted between the sham and sham+atorvastatin groups (Tables 1 and 2, Fig. 2D).

These findings strongly suggested that atorvastatin could slow the progression from hypertrophy to heart failure. We therefore investigated the mechanisms involved.

Atorvastatin Downregulates Expression of MMPs and HB-EGF and BNP

Recent studies have revealed that the activation of MMP2 and MMP9 (20), or MMP3 (21), or ADAM12 (8) and ADAM17 (22, 23) can induce the release of HB-EGF and subsequent EGFR transactivation, while upregulation of the expression of MMPs is reported to be associated with cardiac remodeling (24, 25). In addition, statins are reported to effectively inhibit the activity of MMPs (26, 27). Therefore, we examined cardiac expression of the genes for MMP2, MMP9, BNP, ADAM12 and 17 and HB-EGF in a TAC mouse model. As expected, compared with those in the sham group, the expressions of MMP2, BNP, and HB-EGF were increased by 3- to 5-fold in the TAC group, and atorvastatin markedly downregulated these genes (Fig. 3A–C). ADAM12 and 17 were also upregulated in TAC mice and inhibited by atorvastatin (Fig. 3D). There was no significant change in the MMP9 gene.

Atorvastatin Inhibits Phosphorylation of EGFR and ERK1/2

Since ERK is recognized as one of the downstream elements of the EGFR signaling pathway and there are reports that statins can inhibit ERK activation (28), we examined the effect of atorvastatin on the activity of both EGFR and ERK1/2 in the hearts of mice. In the TAC group, myocardial EGFR and ERK1/2 activity was increased dramatically relative to that in the sham group, while atorvastatin markedly inhibited their activation (Fig. 3E–H).

Atorvastatin Increases the Production of Nitric Oxide

As shown in Fig. 3I, the plasma level of NO_x was markedly decreased in TAC mice at 4 weeks, and was significantly increased in TAC mice treated with atorvastatin.

Atorvastatin Inhibits PE-Induced Protein Synthesis and EGFR Phosphorylation of Cardiomyocytes

In experiments using cultured neonatal rat cardiomyocytes, we found that protein synthesis was enhanced by PE and was dose-dependently inhibited by co-treatment with

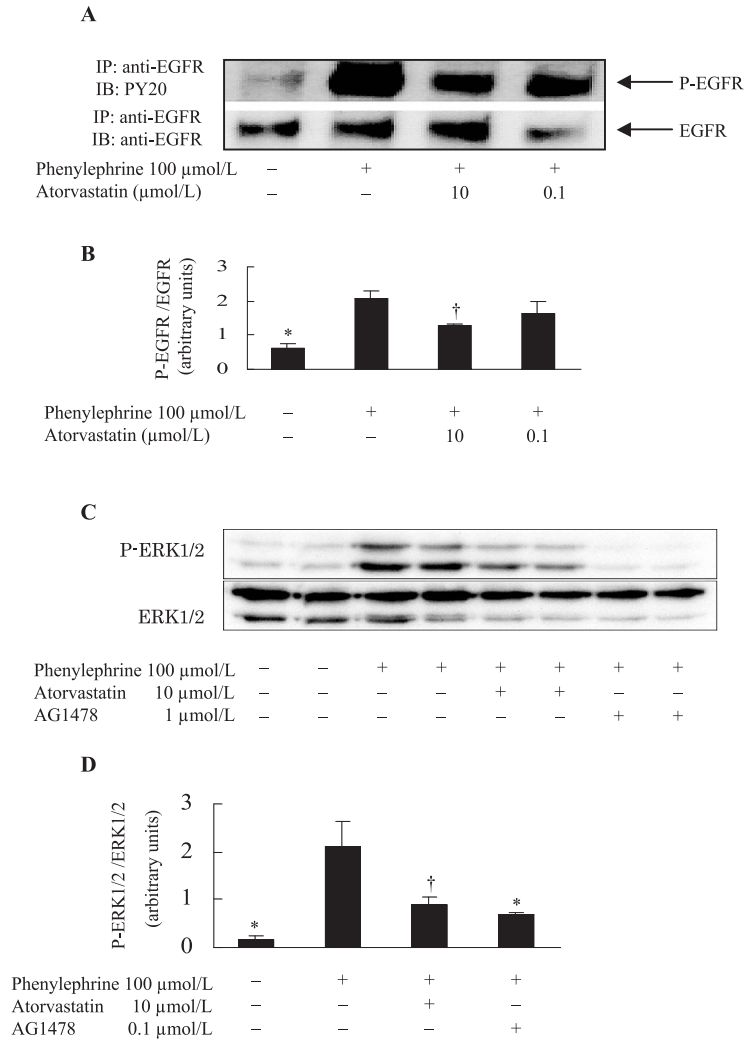


Fig. 5. Atorvastatin inhibited the EGFR-ERK signaling pathway *in vitro*. EGFR phosphorylation induced by phenylephrine was significantly inhibited by atorvastatin (A and B). Atorvastatin or EGFR inhibitor AG1478 attenuated phenylephrine-stimulated ERK1/2 activation (C, D). After 30 min of exposure to atorvastatin or AG1478, phenylephrine was added and incubated for 5 min. Each experiment was repeated at least 3 times. ANOVA $p=0.001$, in both B and D; $*p<0.01$, $^{\dagger}p<0.05$ vs. phenylephrine (Fisher test).

atorvastatin (Fig. 4).

Based on our earlier report that EGFR activation by G-protein-coupled receptor (GPCR) agonists leads to the development of cardiac hypertrophy (8) and the findings that statins could inhibit the increase of cardiomyocyte protein synthesis stimulated by PE or angiotensin II (29), we hypothesized that atorvastatin may inhibit cardiomyocyte hypertrophy by preventing tyrosine phosphorylation of the EGFR. As a result, atorvastatin was found to inhibit EGFR phosphorylation induced by exposure to PE (Fig. 5A, B). In addition, PE induced the activation of ERK1/2, and atorvastatin inhibited that activation (Fig. 5C, D). Furthermore, the EGFR inhibitor AG1478 effectively attenuated PE-induced ERK activity (Fig. 5C, D). These data indicate that atorvastatin targets the

GPCR-EGFR-mitogen-activated protein kinases (MAPKs) signaling pathway.

Discussion

This study demonstrated that atorvastatin could markedly ameliorate cardiac remodeling induced by LV pressure overload. The beneficial effects of atorvastatin observed in this study included a decrease of cardiomyocyte hypertrophy, as well as improvements of pulmonary congestion, cardiac fibrosis, left ventricular contractility (LVFS and LVEF), and left ventricular diastolic indices (LVEDP and τ). We also found that downregulation of MMPs and HB-EGF gene expression along with a reduction of EGFR phosphorylation

and ERK activity, and increase of nitric oxide production were associated with the suppression of cardiomyocyte hypertrophy and improvement of heart failure by atorvastatin.

Our finding that atorvastatin can improve both systolic and diastolic dysfunction is in good agreement with several recent clinical observations (2–5). Considering that a relatively low proportion of patients with non-ischemic heart failure receive statin therapy and a relatively high proportion of CHF patients have diastolic dysfunction, use of statins to treat CHF should be increased.

It is known that EGFR transactivation plays an important role in cardiovascular remodeling (8, 20, 30–32). It has been reported that activation of ADAM12 (8) or ADAM17 (22) could induce the release of HB-EGF and subsequent EGFR phosphorylation, which may eventually lead to cardiomyocyte hypertrophy, while inhibition of ADAM12 or administration of an HB-EGF neutralizing antibody blocked GPCR agonist-stimulated myocyte hypertrophy (8). A study performed by Lucchesi *et al.* supported the existence of a signaling pathway for pressure-induced HB-EGF release and subsequent EGFR activation in murine mesenteric resistance arteries (20). Zhang *et al.* confirmed that a similar pathway is activated to promote smooth muscle cell growth (32). Interestingly, a recent study reported that GPCR modification could inhibit cardiac hypertrophy *via* reduction of EGFR transactivation (33). The present study showed that atorvastatin could substantially decrease cardiac remodeling, as indicated by a reduction of LV wall thickness and LV dimensions as well as improvement of myocyte hypertrophy and perivascular fibrosis, findings that are consistent with the results of a recent pilot clinical trial (4) and several previous experimental studies (28, 29, 34). However, no study has yet examined whether or not statins can inhibit EGFR transactivation. In this study, we obtained evidence that atorvastatin could inhibit EGFR phosphorylation induced by pressure overload or the GPCR agonist PE. Since HB-EGF released from the cell membrane is soluble and the protein expression level is very low, it is not easy to detect by Western blot analysis. Instead, we found that myocardial expression of ADAM12 and 17 and HB-EGF was significantly increased in the presence of cardiac hypertrophy and heart failure, and that atorvastatin dramatically reversed the upregulation of these gene expressions, supporting the possibility that atorvastatin inhibits the MMPs–HB-EGF–EGFR signal pathway. We further confirmed that atorvastatin inhibited PE-induced ERK activation, while inhibition of EGFR by AG1478 dramatically attenuated PE-induced ERK activity, suggesting that ERK is located downstream of the EGFR activation pathway. Our *in vivo* data also showed that atorvastatin suppressed the increase of ERK activity in hypertrophied and failing hearts, which is in agreement with the results of previous studies (28, 35). Notably, this study provided the first direct evidence that *in vivo* phosphorylation increased in hypertrophic and failing hearts.

It should be noted that other actions of atorvastatin might

have contributed to its inhibitory effect on cardiac remodeling in this study, including an antioxidant effect (29, 36), enhancement of nitric oxide availability (37), an antiinflammatory effect (38), and inhibition of neurohormonal activation (39).

In summary, atorvastatin effectively suppressed cardiac remodeling induced by pressure overload in mice, and inhibition of the activation of EGFR and ERK and increase in the nitric oxide production were possible mechanisms involved.

References

1. Yan AT, Yan RT, Liu PP: Narrative review: pharmacotherapy for chronic heart failure: evidence from recent clinical trials. *Ann Intern Med* 2005; **142**: 132–145.
2. Fukuta H, Sane DC, Brucks S, Little WC: Statin therapy may be associated with lower mortality in patients with diastolic heart failure: a preliminary report. *Circulation* 2005; **112**: 357–363.
3. Horwich TB, MacLellan WR, Fonarow GC: Statin therapy is associated with improved survival in ischemic and non-ischemic heart failure. *J Am Coll Cardiol* 2004; **43**: 642–648.
4. Sola S, Mir MQ, Lerakis S, Tandon N, Khan BV: Atorvastatin improves left ventricular systolic function and serum markers of inflammation in nonischemic heart failure. *J Am Coll Cardiol* 2006; **47**: 332–337.
5. Node K, Fujita M, Kitakaze M, Hori M, Liao JK: Short-term statin therapy improves cardiac function and symptoms in patients with idiopathic dilated cardiomyopathy. *Circulation* 2003; **108**: 839–843.
6. Kjekshus J, Dunselman P, Blideskog M, *et al*: A statin in the treatment of heart failure? Controlled rosuvastatin multinational study in heart failure (CORONA): study design and baseline characteristics. *Eur J Heart Fail* 2005; **7**: 1059–1069.
7. Tavazzi L, Tognoni G, Franzosi MG, *et al*: Rationale and design of the GISSI heart failure trial: a large trial to assess the effects of *n*-3 polyunsaturated fatty acids and rosuvastatin in symptomatic congestive heart failure. *Eur J Heart Fail* 2004; **6**: 635–641.
8. Asakura M, Kitakaze M, Takashima S, *et al*: Cardiac hypertrophy is inhibited by antagonism of ADAM12 processing of HB-EGF: metalloproteinase inhibitors as a new therapy. *Nat Med* 2002; **8**: 35–40.
9. Liao Y, Asakura M, Takashima S, *et al*: Benidipine, a long-acting calcium channel blocker, inhibits cardiac remodeling in pressure-overloaded mice. *Cardiovasc Res* 2005; **65**: 879–888.
10. Liao Y, Ishikura F, Beppu S, *et al*: Echocardiographic assessment of LV hypertrophy and function in aortic-banded mice: necropsy validation. *Am J Physiol Heart Circ Physiol* 2002; **282**: H1703–H1708.
11. Youssef S, Stuve O, Patarroyo JC, *et al*: The HMG-CoA reductase inhibitor, atorvastatin, promotes a Th2 bias and reverses paralysis in central nervous system autoimmune disease. *Nature* 2002; **420**: 78–84.
12. Teichholz LE, Kreulen T, Herman MV, Gorlin R: Problems in echocardiographic volume determinations: echocardi-

- graphic-angiographic correlations in the presence of absence of asynergy. *Am J Cardiol* 1976; **37**: 7–11.
13. Iwamoto R, Yamazaki S, Asakura M, *et al*: Heparin-binding EGF-like growth factor and ErbB signaling is essential for heart function. *Proc Natl Acad Sci U S A* 2003; **100**: 3221–3226.
 14. Privratsky JR, Wold LE, Sowers JR, Quinn MT, Ren J: AT1 blockade prevents glucose-induced cardiac dysfunction in ventricular myocytes: role of the AT1 receptor and NADPH oxidase. *Hypertension* 2003; **42**: 206–212.
 15. Asanuma H, Kitakaze M, Node K, *et al*: Benidipine, a long-acting Ca channel blocker, limits infarct size *via* bradykinin- and NO-dependent mechanisms in canine hearts. *Cardiovasc Drugs Ther* 2001; **15**: 225–231.
 16. Kitakaze M, Node K, Minamino T, Asanuma H, Kuzuya T, Hori M: A Ca channel blocker, benidipine, increases coronary blood flow and attenuates the severity of myocardial ischemia *via* NO-dependent mechanisms in dogs. *J Am Coll Cardiol* 1999; **33**: 242–249.
 17. Tatsumi T, Akashi K, Keira N, *et al*: Cytokine-induced nitric oxide inhibits mitochondrial energy production and induces myocardial dysfunction in endotoxin-treated rat hearts. *J Mol Cell Cardiol* 2004; **37**: 775–784.
 18. Liao Y, Takashima S, Asano Y, *et al*: Activation of adenosine A1 receptor attenuates cardiac hypertrophy and prevents heart failure in murine left ventricular pressure-overload model. *Circ Res* 2003; **93**: 759–766.
 19. Liao Y, Asakura M, Takashima S, *et al*: Celiprolol, a vasodilatory beta-blocker, inhibits pressure overload-induced cardiac hypertrophy and prevents the transition to heart failure *via* nitric oxide-dependent mechanisms in mice. *Circulation* 2004; **110**: 692–699.
 20. Lucchesi PA, Sabri A, Belmadani S, Matrougui K: Involvement of metalloproteinases 2/9 in epidermal growth factor receptor transactivation in pressure-induced myogenic tone in mouse mesenteric resistance arteries. *Circulation* 2004; **110**: 3587–3593.
 21. Suzuki M, Raab G, Moses MA, Fernandez CA, Klagsbrun M: Matrix metalloproteinase-3 releases active heparin-binding EGF-like growth factor by cleavage at a specific juxtamembrane site. *J Biol Chem* 1997; **272**: 31730–31737.
 22. Hinkle CL, Sunnarborg SW, Loiselle D, *et al*: Selective roles for tumor necrosis factor alpha-converting enzyme/ADAM17 in the shedding of the epidermal growth factor receptor ligand family: the juxtamembrane stalk determines cleavage efficiency. *J Biol Chem* 2004; **279**: 24179–24188.
 23. Ohtsu H, Dempsey PJ, Eguchi S: ADAMs as mediators of EGF receptor transactivation by G protein-coupled receptors. *Am J Physiol Cell Physiol* 2006; **291**: C1–C10.
 24. Sakata Y, Yamamoto K, Mano T, *et al*: Activation of matrix metalloproteinases precedes left ventricular remodeling in hypertensive heart failure rats: its inhibition as a primary effect of angiotensin-converting enzyme inhibitor. *Circulation* 2004; **109**: 2143–2149.
 25. Moshal KS, Tyagi N, Moss V, *et al*: Early induction of matrix metalloproteinase-9 transduces signaling in human heart end stage failure. *J Cell Mol Med* 2005; **9**: 704–713.
 26. Nicholls SJ, Cutri B, Worthley SG, *et al*: Impact of short-term administration of high-density lipoproteins and atorvastatin on atherosclerosis in rabbits. *Arterioscler Thromb Vasc Biol* 2005; **25**: 2416–2421.
 27. Fukumoto Y, Libby P, Rabkin E, *et al*: Statins alter smooth muscle cell accumulation and collagen content in established atheroma of watanabe heritable hyperlipidemic rabbits. *Circulation* 2001; **103**: 993–999.
 28. Patel R, Nagueh SF, Tsybouleva N, *et al*: Simvastatin induces regression of cardiac hypertrophy and fibrosis and improves cardiac function in a transgenic rabbit model of human hypertrophic cardiomyopathy. *Circulation* 2001; **104**: 317–324.
 29. Takemoto M, Node K, Nakagami H, *et al*: Statins as antioxidant therapy for preventing cardiac myocyte hypertrophy. *J Clin Invest* 2001; **108**: 1429–1437.
 30. Thomas WG, Brandenburger Y, Autelitano DJ, Pham T, Qian H, Hannan RD: Adenoviral-directed expression of the type 1A angiotensin receptor promotes cardiomyocyte hypertrophy *via* transactivation of the epidermal growth factor receptor. *Circ Res* 2002; **90**: 135–142.
 31. Kagiya S, Eguchi S, Frank GD, Inagami T, Zhang YC, Phillips MI: Angiotensin II-induced cardiac hypertrophy and hypertension are attenuated by epidermal growth factor receptor antisense. *Circulation* 2002; **106**: 909–912.
 32. Zhang H, Chalothorn D, Jackson LF, Lee DC, Faber JE: Transactivation of epidermal growth factor receptor mediates catecholamine-induced growth of vascular smooth muscle. *Circ Res* 2004; **95**: 989–997.
 33. Zhai P, Galeotti J, Liu J, *et al*: An angiotensin II type 1 receptor mutant lacking epidermal growth factor receptor transactivation does not induce angiotensin II-mediated cardiac hypertrophy. *Circ Res* 2006; **99**: 528–536.
 34. Nadruz W Jr, Lagosta VJ, Moreno H Jr, Coelho OR, Franchini KG: Simvastatin prevents load-induced protein tyrosine nitration in overloaded hearts. *Hypertension* 2004; **43**: 1060–1066.
 35. Miura S, Matsuo Y, Saku K: Simvastatin suppresses coronary artery endothelial tube formation by disrupting Ras/Raf/ERK signaling. *Atherosclerosis* 2004; **175**: 235–243.
 36. Morikawa-Futamatsu K, Adachi S, Maejima Y, *et al*: HMG-CoA reductase inhibitor fluvastatin prevents angiotensin II-induced cardiac hypertrophy *via* Rho kinase and inhibition of cyclin D1. *Life Sci* 2006; **79**: 1380–1390.
 37. Landmesser U, Engberding N, Bahlmann FH, *et al*: Statin-induced improvement of endothelial progenitor cell mobilization, myocardial neovascularization, left ventricular function, and survival after experimental myocardial infarction requires endothelial nitric oxide synthase. *Circulation* 2004; **110**: 1933–1939.
 38. Rosenson RS, Tangney CC, Casey LC: Inhibition of proinflammatory cytokine production by pravastatin. *Lancet* 1999; **353**: 983–984.
 39. Pliquett RU, Cornish KG, Peuler JD, Zucker IH: Simvastatin normalizes autonomic neural control in experimental heart failure. *Circulation* 2003; **107**: 2493–2498.